

# Multiwave COVID-19 Prediction via Social Awareness-Based Graph Neural Networks using Mobility and Web Search Data

Jiawei Xue  
xue120@purdue.edu  
Purdue University  
West Lafayette, IN, USA

Takahiro Yabe  
tyabe@mit.edu  
Massachusetts Institute of Technology  
Cambridge, MA, USA

Kota Tsubouchi  
ktsubouc@yahoo-corp.jp  
Yahoo Japan Corporation  
Tokyo, Japan

Jianzhu Ma\*  
majianzhu@pku.edu.cn  
Peking University  
Beijing, China

Satish V. Ukkusuri\*  
sukkusur@purdue.edu  
Purdue University  
West Lafayette, IN, USA

## ABSTRACT

Recurring outbreaks of COVID-19 have posed enduring effects on global society, which calls for a predictor of pandemic waves using various data with early availability. Existing prediction models that forecast the first outbreak wave using mobility data may not be applicable to the multiwave prediction, because the evidence in the USA and Japan has shown that mobility patterns across different waves exhibit varying relationships with fluctuations in infection cases. Therefore, to predict the multiwave pandemic, we propose a Social Awareness-Based Graph Neural Network (SAB-GNN) that considers the decay of symptom-related web search frequency to capture the changes in public awareness across multiple waves. SAB-GNN combines GNN and LSTM to model the complex relationships among urban districts, inter-district mobility patterns, web search history, and future COVID-19 infections. We train our model to predict future pandemic outbreaks in the Tokyo area using its mobility and web search data from April 2020 to May 2021 across four pandemic waves collected by ANONYMOUS\_COMPANY under strict privacy protection rules. Results show our model outperforms other baselines including ST-GNN and MPNN+LSTM. Though our model is not computationally expensive (only 3 layers and 10 hidden neurons), the proposed model enables public agencies to anticipate and prepare for future pandemic outbreaks.

## 1 INTRODUCTION

The spreading mechanism of COVID-19 [27] is complicated due to its dependency on disease features and social factors such as human mobility [34, 51], public awareness[35], and intervention policies [12]. One prominent phenomenon of the complex disease spreading process is the multiple outbreak wave, which implies the periodic rebound to a large number of infection cases [3, 24, 29] and is obvious in many countries such as the USA, UK, France, and Japan (Figure 1). Abrupt and uncertain disease outbreaks disturb individuals' daily life, government's reopening policies [5], medical resources managements [30], and risk assessment [56]. It has an

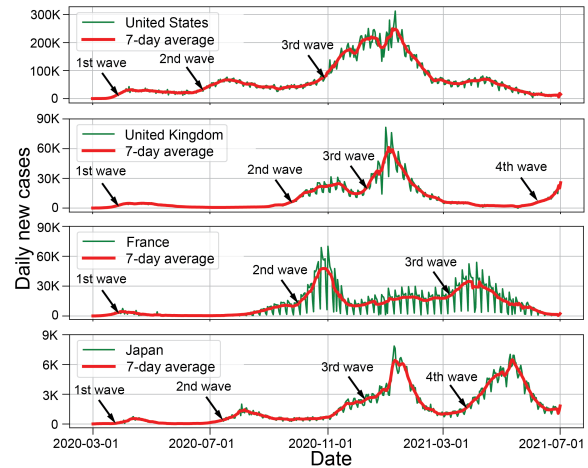


**Figure 1: The daily new infection cases of COVID-19 for four countries [15]. We observe multiple pandemic waves with varying starting days and magnitudes.**

enormous social impact to investigate and construct such an accurate model to predict the multiple waves by fully utilizing different types of social and mobility data [48].

Many prediction models for the first outbreak wave have been proposed to anticipate the infection and death cases [9, 28, 40, 41]. One critical input for these models is the mobility data [6, 19, 22], which describes population movements and is positively related to the disease infections [49]. Nevertheless, continuous tracking of human mobility dynamics shows that the mobility strength did not exhibit consistent relationships with infection cases: (1) the USA: human mobility fluctuated around 95% of the normal period from July 1 to Dec. 1, 2020 [10] which witnessed the second wave in July and the third wave in November (Figure 1); (2) Tokyo: the social contact index resumed to the normal level and decreased slightly after July 2020, but Tokyo experienced the second wave since then [52]. The inconsistency in the mobility strength and disease infection necessitates other data that is more representative of disease outbreak waves.

During COVID-19, many text-based methods have been proposed to aid communities such as to understand human’s emotion states [21] and to answer peoples’ questions [53]. Web search records collected by the web service provider have extensive applications such as customer behavior analysis [14], stock market prediction [58], and disease outbreak monitoring [2, 17]. For COVID-19, symptom-related web search records (e.g., *fever*, *cough*, and *headache*) reflect the public’s virus-induced symptoms that cannot be mined from the mobility data. Evidence in Tokyo showed that the Pearson correlation between *High-Risk Users* (which are defined from web search records) and infection cases was 0.719 with a 16-day lag for the second wave [52]. It also found people’s symptom-related web search frequency was smaller during the second wave than the first wave, though the number of patients were significantly higher. These results inspire us to leverage the web search data and recover human awareness decay to predict the multiwave pandemic.

In this study, we propose a multiwave infection prediction approach, with the direct application as urban district-level disease outbreak early warning. District-level disease prediction has the following three requirements: (1) comprehensive data sources, such as people movement and social responses, should be included to contain various hints that are closely related to the disease spreading; (2) spatial and temporal disease dissemination patterns of COVID-19 should be taken into consideration; (3) it captures complex dependency between infection cases and other factors. To deal with these challenges, we first define the Web search-Mobility Network (WMN) whose nodes and edges maintain web search frequency and inter-district trip information, respectively. Afterward, we propose a Social Awareness-Based Graph Neural Network (SAB-GNN) architecture upon the WMN to capture the spatio-temporal infection case dynamics in different urban districts. We train and test the model using real-world infection, human mobility, and web search data in the Tokyo area from April 2020 to May 2021, and obtain better prediction performance than baseline models. Our method has three contributions:

- We focus on predicting multiwave disease outbreaks that are globally prevalent but are seldom investigated. Different from a single wave prediction, multiwave prediction enables the public agencies to evaluate the long-term risk and take appropriate actions at different pandemic stages.
- We propose the SAB-GNN by fusing historical infection, mobility, and web search data that provide sufficient evidence of potential disease outbreaks. The spatial module, temporal module, and social awareness module take separate responsibilities and jointly contribute to the final prediction.
- The proposed method is implemented on a mega-city, Tokyo, with a period spanning more than one year across four pandemic waves. We conduct a comprehensive analysis of disease outbreaks and prediction results from different models at different time intervals, which promotes a more nuanced understanding of the disease waves.

## 2 RELATED WORK

**Time series models:** Existing COVID-19 time series models cover multiple types such as auto-regressive integrated moving average

(ARIMA) [28], and long short-term memory (LSTM) [9, 20]. Moreover, biologists and engineering scientists focus on the relationship between fatality rate and biochemical indicators [59], human mobility [20]. When it comes to urban district-level disease infection prediction, while the inter-district connections provide crucial pathways for both human movement and disease dissemination, these models are insufficient to capture such spatial dependency between different urban districts. In fact, the spatial dependency information enables us to deal with the data scarcity issue which may occur during the pandemic season. For instance, assume that we have sufficient mobility and social media data for district  $\mathcal{A}$  and deficient data for district  $\mathcal{B}$ , and recognize strong mobility connections between districts  $\mathcal{A}$  and  $\mathcal{B}$ . Considering the connections between the two districts helps to fully utilize the infection information and predict the infection cases in a global manner.

**Graph neural networks:** Graph neural network (GNN) is an innovative neural network that captures the relationship between multi-hop neighborhood nodes via the message passing mechanism [60]. In the past years, various GNN models such as graph convolutional network (GCN) [26], GraphSage [16], graph attention network (GAT) [43], and relational graph convolutional network (R-GCN) [39] were developed and applied to many fields such as neural machine translation [1], visual question answering [31], traffic prediction [7, 33, 46, 54, 57], network metric generation [50], and online diagnosis [47].

Researchers have harnessed the superiority of the GNN in modeling spatial dependency to perform the disease infection case prediction. Most published GNN approaches [13, 23, 32] focused on the infection prediction before July 2020 when the first global outbreak occurred using the historical infection and mobility data. The mobility data was sufficient to reflect the disease spreading patterns during the first wave thanks to its simple relationship with the infection. First, areas attracting more passengers had higher risks of experiencing rapidly increasing cases than some lonely areas at the beginning of the first wave. Second, the travel restriction policies during the first wave suppressed the mobility strength and thus decelerated the disease outbreak [49].

Nevertheless, the interaction between infection and mobility evolved into a much more complicated status during the later waves because the infection cases were affected by a large variety of causes such as mask policy, the vaccination, which hindered the ability of pure mobility data to reflect the infection tendency. In addition, many studies have recognized that the available mobility data for COVID-19 infection cases prediction was limited by the period length [32, 37], which resulted in unstable learned models. In summary, the long-term multiwave infection prediction requests alternative data sources that provide sufficient interconnections with the infection case under the dynamic environment. In this study, we turn to the novel web search data, which directly reveals human’s awareness to the disease and potential symptoms, to perform the multiwave disease prediction.

## 3 PRELIMINARIES

In this section, we first describe the mobility and web search data used as features for the prediction, and then formally define our prediction task. Consider an urban area that is divided into several

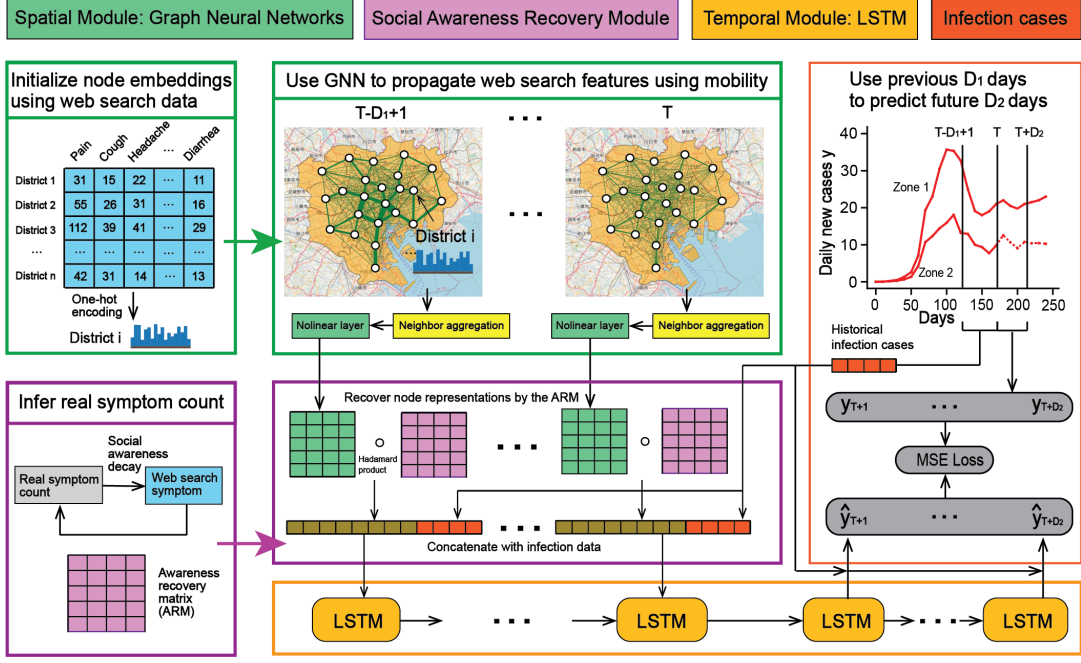


**Figure 2: The framework of Social Awareness-Based Graph Neural Networks.** We first model urban districts as nodes, and propagate the web search frequency embedding using the mobility information. Then, we use a learnable social awareness matrix to recover node representations, and feed them into an LSTM sequence to predict the next  $D_2$  days’ infection cases.

pre-defined urban districts. For the mobility data, we first collect location records (longitude, latitude, and time) of mobile phone users within the urban area and extract each individual’s trajectory points as a sequence. Next, we project the sequence points of each mobile phone user into the urban districts to obtain the number of daily inter-district trips. Note that inter-district trips build natural pathways to transmit disease viruses in the city so that these districts have correlated exposure to disease outbreak risks. For the web search data, we scope  $n_w$  COVID-19 symptom-related web search words from multiple official sources. We assign each mobile phone user to the urban district where his/her home is located and then aggregate the daily web searching frequency for all users living in this district. In summary, we obtain the number of inter-district trips between every two districts, and symptom-related web search frequency in each district for each day.

Our goal is to utilize the infection, mobility, and web search data for the past  $D_1$  days to predict new infection cases for the next  $D_2$  days at the urban district level. We define a sequence of WMNs:  $G_t = (V, E_t, H_t, I_t)$ . Here, the subscript  $t$  implies a day.  $V = \{v_1, v_2, \dots, v_n\}$  represents  $n$  urban districts.  $E_t \in \mathbb{R}^{n \times n}$  is a matrix where the  $(i, j)$ -entry represents the number of trips from the district  $v_i$  to  $v_j$  on the day  $t$ . We denote the daily web search frequency of residents living in the district  $v_i$  as a vector  $\mathbf{h}_t^{v_i} \in \mathbb{R}^{n_w}$  so that  $\mathbf{H}_t = [\mathbf{h}_t^{v_1}, \mathbf{h}_t^{v_2}, \dots, \mathbf{h}_t^{v_n}]^T \in \mathbb{R}^{n \times n_w}$  is the node feature matrix encoding the web search frequency for all districts.  $\mathbf{I}_t \in \mathbb{R}^{n \times 1}$  is the collection of daily new infection cases in different districts.

**Prediction task:** On the day  $T$ , given  $G_t$  for all  $t \in [T-D_1+1, T]$ , predict  $\mathbf{I}_t$  for all  $t \in [T+1, T+D_2]$ .

#### 4 SOCIAL AWARENESS-BASED GRAPH NEURAL NETWORKS

In this section, we first present the intuition of the SAB-GNN model, and then sequentially introduce its three modules: the spatial information propagation module, the social awareness recovery module, and the temporal information passing module, and finally declare the loss function.

We deduce that the future reported district-level infection cases are jointly influenced by the existing infection cases, the number of susceptible individuals that may have been infected (which can be mined from public’s symptom-related web search data), and in-person contact patterns across the city (which is reflected by the inter-district trip numbers) and use them as features. Given that the pandemic spreading is indeed a complicated temporal process embedding on the space, we propose to build temporal and spatial modules [55] to track the infection dynamics. Lastly, the existing study finds that the public’s symptom-related web search frequency decreases from the first wave to the second wave, which reveals a prevalent social phenomenon that people’s awareness of a hot topic gradually declines (which is referred to as *social awareness decay* in this study) [52]. Based on the fact that people adapt themselves to the mask policies, travel restrictions, and routine testings and pay less attention to the COVID-19, we propose a social awareness recovery module in the SAB-GNN to estimate the actual occurrence of COVID-19-related symptoms. Taken together, we build an integrated future infection case prediction model with three modules (i.e., spatial module, awareness recovery module, and temporal

module) by fusing the historical infection, mobility, and web search data.

#### 4.1 Spatial Module: Graph Neural Networks

Recall that the web search frequency vector  $\mathbf{h}_t^{v_i}$  reflects the number of potential infected individuals in the urban district  $v_i$  and  $\mathbf{E}_t$  records the daily inter-district trips. We therefore perform the convolution operation on  $\mathbf{h}_t^{v_i}$  using the  $\mathbf{E}_t$  information under the graph neural network framework to capture the disease risk propagation properties. As shown in Figure 2, using the symptom-related web search frequency in each urban district, we employ the one-hot encoding to initialize the representation for each urban district (i.e., each node in  $G_t$ ) as the input matrix:  $\mathbf{X}_t^{(0)} = \mathbf{H}_t$ . Following the GCN model [26], we define the node representation propagation rule between the layers  $k$  and  $(k + 1)$  as:

$$\mathbf{X}_t^{(k+1)} = \sigma(\tilde{\mathbf{D}}_t^{-\frac{1}{2}} \tilde{\mathbf{E}}_t \tilde{\mathbf{D}}_t^{-\frac{1}{2}} \mathbf{X}_t^{(k)} \mathbf{W}^{(k)}), \quad (1)$$

where

$$\tilde{\mathbf{E}}_t = \mathbf{E}_t + \mathbf{I}_{n \times n}, \tilde{\mathbf{D}}_{ii} = \sum_{j=1}^n \tilde{\mathbf{E}}_{ij}, \quad (2)$$

and  $\mathbf{W}^{(k)}$  is a learnable weight matrix,  $\mathbf{I}_{n \times n}$  is the  $n$  by  $n$  identity matrix,  $\sigma(\cdot)$  is the activation function ReLU.

Note that we normalize the matrix  $\mathbf{E}_t$  such that the sum of each column is equal to 1 (i.e., the sum of incoming edges on one node is 1), which is used in the existing study [32]. In practice, it is possible to replace the spectral convolution with other GNN variants such as GAT, GraphSage. We also implement them and find quite approximate prediction performance as the GCN. The outcome of the spatial module is a matrix

$$\mathbf{H}_t^S = \mathbf{X}_t^{(K)} = [\mathbf{x}_t^{v_1}, \mathbf{x}_t^{v_2}, \dots, \mathbf{x}_t^{v_n}]^T, \quad (3)$$

with  $n$  rows that encode the web search frequency and mobility where  $K$  is the number of layers.

#### 4.2 Social Awareness Recovery Module

The symptom-related web search frequency is positively related to the number of actual symptom occurrences among the population, as well as the probability that a user with a symptom searches the word on the Internet. As mentioned earlier, the social awareness decay effect informs that probability of symptom-related word searching gradually decreases with time after the first COVID-19 wave. To estimate the actual symptom occurrences, we propose to multiply the observed web search representation by a monotonically increasing function with respect to the time.

Specifically, we first linearly normalize each entry of the web search record vector  $\mathbf{h}_t^{v_i}$  to 0 and 1 by the maximal and minimal web search frequency of each word across all days in the urban district  $v_i$ , and feed them into the spatial module, and obtain  $\mathbf{H}_t^S$ . Next, we define a simple increasing function  $r(t|i, t_0) = e^{\lambda_i^2(t-t_0)}$  regarding  $t$  to recover the social awareness:

$$\tilde{\mathbf{x}}_t^{v_i} = \mathbf{x}_t^{v_i} r(t|i, t_0) = \mathbf{x}_t^{v_i} e^{\lambda_i^2(t-t_0)}, \quad (4)$$

where  $\lambda_i^2$  is learnable and measures the social awareness recovery rate in  $v_i$ .  $t$ ,  $t_0$  represent the current day and the first day of the study period, respectively. Given that the land use, economy

type, demographic characteristic discrepancy may lead to spatially varying social awareness rates, we specify district-dependent  $\lambda_i^2$  to encode its unique awareness decay behavior. A large value of  $\lambda_i^2$  implies that social awareness of COVID-19 for residents living in  $v_i$  declines rapidly and we therefore adopt this large value to recover the social awareness. Note that we introduce the square in  $\lambda_i^2$  to ensure that it is non-negative. Collectively speaking, the social awareness recovery module transforms  $\mathbf{H}_t^S$  to  $\tilde{\mathbf{H}}_t^S$  by

$$\tilde{\mathbf{H}}_t^S = \mathbf{H}_t^S \circ \mathbf{M}_{t,t_0}, \quad (5)$$

where  $\mathbf{M}_{t,t_0}$  is the awareness recovery matrix (ARM):

$$\mathbf{M}_{t,t_0} = \begin{bmatrix} e^{\lambda_1^2(t-t_0)} & e^{\lambda_1^2(t-t_0)} & \dots & e^{\lambda_1^2(t-t_0)} \\ e^{\lambda_2^2(t-t_0)} & e^{\lambda_2^2(t-t_0)} & \dots & e^{\lambda_2^2(t-t_0)} \\ \vdots & \vdots & \ddots & \vdots \\ e^{\lambda_n^2(t-t_0)} & e^{\lambda_n^2(t-t_0)} & \dots & e^{\lambda_n^2(t-t_0)} \end{bmatrix}, \quad (6)$$

and  $\circ$  is the Hadamard product. This transform implies that the entries in  $\mathbf{H}_t^S$  are amplified to capture the actual disease risk which is underestimated due to the social awareness decay effect when  $t$  is large. In the end, we perform 0-1 normalization on the infection matrix  $\mathbf{I}_t$  to obtain  $\tilde{\mathbf{I}}_t$ , and arrive at the output of the social awareness recovery module by concatenating the web search and infection representations, which is

$$\mathbf{H}_t^A = [\tilde{\mathbf{H}}_t^S, \tilde{\mathbf{I}}_t]. \quad (7)$$

#### 4.3 Temporal Module: Long Short-Term Memory

To capture the temporal dependency of district-level features and infection cases, we adopt the existing LSTM model [18].  $\forall i \in 1, 2, \dots, n$ , we extract the  $i$ -th row of matrices  $\mathbf{H}_t^A$ ,  $t \in [T - D_1 + 1, T]$  and feed them into an LSTM sequence (Figure 2). Since we have already modelled the spatial dependency in the spatial module, in the temporal module we pass the node representations from  $\mathbf{H}_t^A$  separately for different nodes, and these LSTM sequences share the identical structures and parameters.

#### 4.4 Loss Function

Recall that our objective is to perform the infection case prediction for the next  $D_2$  days, we define the loss function as the mean squared error, which is:

$$\mathcal{L}_T = \frac{1}{D_2 n} \sum_{t=T+1}^{T+D_2} \sum_{i=1}^n (I_{t,i} - \hat{I}_{t,i})^2, \quad (8)$$

where  $I_{t,i}$  and  $\hat{I}_{t,i}$  denote the actual and predicted infection cases for the district  $i$  on the day  $t$ . We present the training process as Algorithm 1.

### 5 EXPERIMENTS

#### 5.1 Mobility, Web Search, and Symptom Data

We utilize four datasets: infection cases, mobile phone location data, web search data, and symptom data in Tokyo from Jan. 6, 2020, to May 15, 2021. The mobility and web search data were owned by an \_ANONYMOUS\_COMPANY\_ with strict privacy protection regulations. The descriptions of these data are as follows:

**Algorithm 1** Training algorithm of SAB-GNN

**Require:**  $\{G_t, T - D_1 + 1 \leq t \leq T; I_t, T + 1 \leq t \leq T + D_2\}_{T \in T_{train}}$ ,  
 where  $G_t = (V, E_t, H_t, I_t)$ .

**Ensure:** the SAB-GNN model.

```

1: for each epoch do
2:   for each batch do
3:      $\mathcal{L}_{batch} \leftarrow 0, m = 0;$ 
4:     for  $T$  in this batch do
5:        $m \leftarrow m + 1;$ 
6:       /* Spatial module */
7:       Evaluate  $X_t^{(k+1)}$  using Eq. (1),  $T - D_1 + 1 \leq t \leq T$ ;
8:       Generate representations
9:        $H_t^S = X_t^{(K)}, T - D_1 + 1 \leq t \leq T$ ;
10:      /* Social awareness recovery module */
11:      Update  $H_t^S$  with  $M_{t,t_0}$ ;
12:      Compute  $H_t^A$  using Eq. (7);
13:      /* Temporal module */
14:      Feed each row  $i$  of  $H_t^A$  into an LSTM model and
15:      obtain the hidden states for  $t = T + 1, T + 2, \dots, T + D_2$ ;
16:      Use a one-layer perceptron to transform
17:      these hidden states to  $D_2$  predicted cases  $\hat{I}_{t,i}$ ;
18:      Compute the loss  $\mathcal{L}_T$  using Eq. (8);
19:       $\mathcal{L}_{batch} \leftarrow \frac{m-1}{m} \mathcal{L}_{batch} + \frac{1}{m} \mathcal{L}_T$ ;
20:     end for
21:     Use Adam to update the model.
22:   end for
23: end for

```

- Infection data. We access the daily new infection cases for 23 wards of Tokyo from the Tokyo COVID-19 Task Force website [42] which is maintained by Tokyo metropolitan government.
- Mobility data. Table 1 presents a sample piece of raw mobility data. The mobility data consists of a fake id (after privacy protection operations), the user’s geolocation in terms of longitude and latitude at a specific time. The data collection frequency was around half an hour on average, which depends on the movements of the user: the frequency is higher if the user moves faster. In this study, the mobility data is utilized to identify Tokyo residents’ home locations and mine the Mobility Matrix  $E_t$ .
- Web search data. Table 2 presents a sample piece of raw web search records. Each record contains the user ID, web query words, as well as web search time. The web search data is used to get COVID-19 symptom-related web search counts. Note that the \_ANONYMOUS\_COMPANY\_ maintains these data to promote users’ experiences and does not share any individual-level data with other agencies.
- Symptom data. Based on two existing COVID-19 symptom studies [38, 44] and the COVID-19 symptom list released by the Centers for Disease Control and Prevention [4], we finally specify 44 symptoms, which are used to measure the counts of symptom-related web search records. The full list of these symptoms is shown in Table 3. Note that we translate

these symptoms from English to Japanese, and then count the number of corresponding web searches.

Location data	Sample
ID1	thisisfakeid
Lat	35.683
Lon	139.763
Time (unixtime)	1584390800
Date	20200317

Table 1: A sample of mobility data.

Web search data	Sample
ID1	thisisfakeid
Time	2020-03-17 08:32:14
Query	XXX

Table 2: A sample of web search data.

	Symptom		Symptom
1	Abdominal pain	23	Hot flush
2	Ageusia	24	Hyperhidrosis
3	Anosmia	25	Insomnia
4	Anxiety	26	Lethargic
5	Arthralgia	27	Loss of appetite
6	Body ache	28	Mental health symptoms
7	Chest pain	29	Migraine
8	Chest tightness	30	Nasal dryness
9	Chills	31	Nausea
10	Confusion	32	Oropharyngeal pain
11	Cough	33	Pain
12	Dehydration	34	Palpitation
13	Diarrhea	35	Pyrexia
14	Disorientation	36	Rash
15	Dizziness	37	Rhinorrhea
16	Dyspnea	38	Sinusitis
17	Ear infection	39	Sleep disturbance
18	Ear pain	40	Sneezing
19	Eye infection	41	Stress
20	Eye pain	42	Sweating
21	Fatigue	43	URTI
22	Headache	44	Vomiting

Table 3: Specified COVID-19 related symptoms.

## 5.2 Data Preprocessing

Recall that our prediction task requires the standard mobility matrix  $E_t$  as well as the web search matrix  $H_t$  on the day  $t$ , we design a data preprocessing framework to convert the raw mobility and web search data to  $E_t$  and  $H_t$  (Figure 3). We notice from the raw mobility data that a proportion of user IDs only appear a few times, which

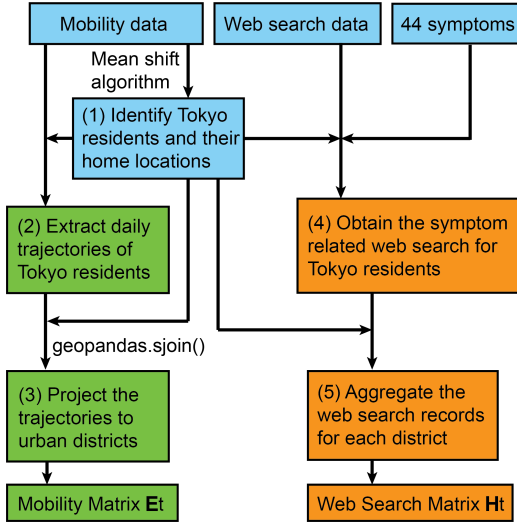


**Figure 3: Data preprocessing framework to obtain inputs for machine-learning models.**

indicates that they might be contemporary travelers in Tokyo and may not be strongly related to the inter-city disease spreading in several months, and thus exclude their mobility data in this study. We finally identify 551,745 permanent users in the 23 special wards of Tokyo, which take around 6% of the total population in these wards. Our mobility and web search data preprocessing procedure is as follows:

- We apply the Mean shift algorithm [8] to each permanent users' location points during the night hours (from 6:00 PM to 9:00 AM) from Jan. 6 to 31, 2020 to estimate the longitude and latitude of their homes using Java (step (1) in Figure 3).
- We extract the daily trajectories of these permanent residents using Java (step (2) in Figure 3) and then project the location points along the trajectories to the urban districts using the spatial join function in geopandas package in Python and obtain the mobility matrix  $E_t$  (step (3) in Figure 3). Note that we mine the daily location trajectory of each user ID and identify cross-district trips with the duration of at least 10 minutes (these trips are referred to as valid trips).
- Based on the specified 44 COVID-19 symptoms, we count the number of symptom searches for each permanent resident using Java (step (4) in Figure 3), aggregate them by urban districts (step (5) in Figure 3), and arrive at the web search matrix  $H_t$ .

The statistics of these data are shown in Figure 4.

### 5.3 Experiment Setting, Evaluation Metrics, Baselines

We conduct experiments to predict two outbreak waves, i.e., **the third wave** (from Dec. 10, 2020 to Feb. 7, 2021) and **the fourth wave** (from March 17 to May 15, 2021). The period for each experiment covers 10 months of observations where the train/validation/test ratio is 70%/10%/20%. We use the first 8 months (months 1 to 8) as training and validation data, and the last 2 months (months 9 and 10)

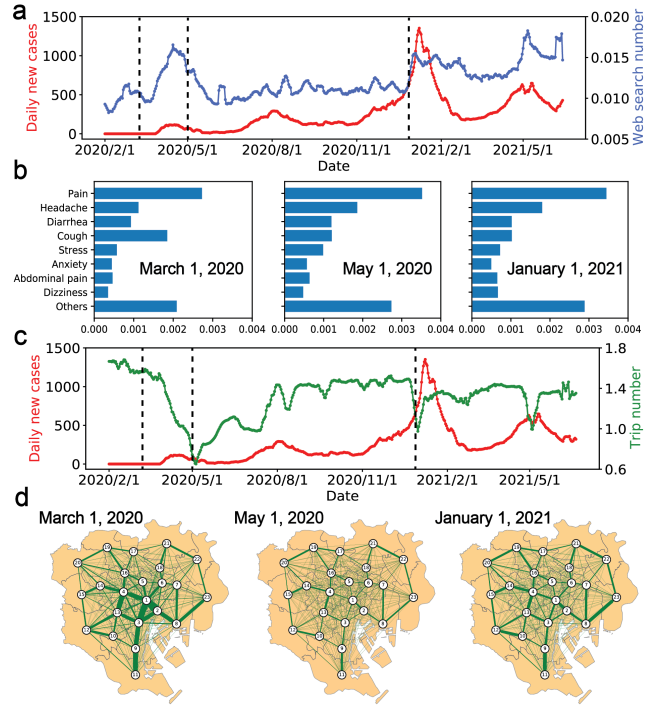


**Figure 4: Statistics of mobility, web search frequency, and infection cases. (a) Dynamics of daily new cases and symptom-related web search frequency per user. (b) The distribution of web search frequency per user on three days. (c) Dynamics of daily new cases and inter-district trip number per user. (d) The number of inter-district trips on three days.**

as testing data. Note that the validation data has the size of 1 month and is evenly distributed from months 7 to 8. Since most existing disease prediction studies [32, 37, 45] predict the infection at the week-level, we design three scenarios:  $(D_1, D_2) = (21, 7), (21, 14), (21, 21)$  (recall that we use the past  $D_1$  days' features to predict the future  $D_2$  days' infection cases).

We train the model using PyTorch and Adam optimizer [25]. We use the validation set to determine the learning rate as 0.0001, the epoch number, the batch size, and the dropout rate as 100, 8, and 0.50, respectively. The experiments run on an Intel Xeon w-2155 3.3 GHz CPU and 32 GB of RAM. Root Mean Square Error (RMSE) and Mean Absolute Error (MAE) are utilized to evaluate the prediction performance:  $RMSE = \sqrt{\frac{1}{D_2 n} \sum_{t=T+1}^{T+D_2} \sum_{i=1}^n (I_{t,i} - \hat{I}_{t,i})^2}$ ,  $MAE = \frac{1}{D_2 n} \sum_{t=T+1}^{T+D_2} \sum_{i=1}^n |I_{t,i} - \hat{I}_{t,i}|$ .

To benchmark our model, we also implement eight existing prediction models: (1) Historical average (HA) infection cases until the day  $T$ ; (2) Historical average of the last  $D_1$  days; (3,4) LSTM; (5,6) Seq2seq: encode the input infection case and decode the sequence using two separate LSTMs [11]; (7) ST-GNN: an Spatio-Temporal GNN model whose inputs are past infection cases and mobility patterns [23]; (8) MPNN+LSTM: a message passing neural network with the LSTM [32].



The Third Wave	Features	$(D_1, D_2) = (21, 7)$		$(D_1, D_2) = (21, 14)$		$(D_1, D_2) = (21, 21)$	
		MAE	RMSE	MAE	RMSE	MAE	RMSE
HA (past all days)	I	22.63	26.45	22.53	27.22	22.16	27.65
HA (past $X$ days)	I	14.15	17.02	16.92	20.72	19.14	23.81
LSTM	I	19.67	24.07	17.23	21.93	20.61	26.61
LSTM	I+W	20.61	24.89	20.72	25.91	19.93	25.94
Seq2seq	I	17.27	22.24	23.04	28.73	16.79	22.77
Seq2seq	I+W	15.69	19.83	21.76	27.46	19.66	25.69
ST-GNN	I+W+M	20.20	25.86	21.53	27.32	20.24	26.36
MPNN+LSTM	I+W+M	12.40	17.31	16.30	21.73	19.78	25.59
SAB-GNN-wsa	I+W+M	10.75	13.43	12.72	16.33	15.61	20.10
SAB-GNN	I+W+M	<b>8.03</b>	<b>10.43</b>	<b>11.23</b>	<b>14.78</b>	<b>13.76</b>	<b>18.24</b>
The Fourth Wave	Features	$(D_1, D_2) = (21, 7)$		$(D_1, D_2) = (21, 14)$		$(D_1, D_2) = (21, 21)$	
		MAE	RMSE	MAE	RMSE	MAE	RMSE
HA (past all days)	I	8.76	10.04	9.14	10.59	9.41	11.08
HA (past $X$ days)	I	4.52	5.76	5.52	7.02	6.47	8.23
LSTM	I	5.94	7.67	8.20	10.64	8.32	10.95
LSTM	I+W	7.43	9.79	8.28	10.55	8.11	10.63
Seq2seq	I	6.37	8.38	8.84	11.42	8.45	11.08
Seq2seq	I+W	5.96	7.74	7.93	9.86	10.43	12.94
ST-GNN	I+W+M	5.46	6.95	7.63	9.97	10.54	13.96
MPNN+LSTM	I+W+M	3.34	4.49	5.27	7.97	<b>4.80</b>	<b>6.56</b>
SAB-GNN-wsa	I+W+M	3.32	4.46	4.63	6.18	5.03	6.77
SAB-GNN	I+W+M	<b>3.25</b>	<b>4.24</b>	<b>4.28</b>	<b>5.57</b>	5.25	6.82

**Table 4: Performance evaluation using past  $D_1$  days’ features to predict next  $D_2$  days’ infection ( $I$ : infection data;  $W$ : web search data;  $M$ : inter-district mobility data; SAB-GNN-wsa: the SAB-GNN model without the social awareness recovery).**

#### 5.4 Comparisons with Baseline Models

We present the prediction performance of the SAB-GNN and other baseline models for the third wave and the fourth wave (Table 4). Our proposed SAB-GNN and SAB-GNN-wsa (without social awareness recovery) models yield the smallest MAE and RMSE for most scenarios (5 out of 6), which demonstrates our models capture the relationships between past infection, web search, mobility, and future infection. Comparing SAB-GNN and SAB-GNN-wsa, the social awareness recovery mechanism decreases the prediction error for most cases (5 out of 6), and the web search frequency has higher predictability after the awareness recovery operation.

In addition, results from all models reveal a general tendency that the web search and mobility features result in prediction performance improvement, even if the past infection case is already a strong feature to connect with the future infection case. Finally, we observe from the LSTM and Seq2seq that simply concatenating the web search frequency embedding with the past infection cases is unable to consistently boost the prediction, which affirms the essentiality of designing a suitable model architecture to utilize the web search data. For each model in Table 1, the running time for each scenario is within 20 minutes on the Ubuntu system with 32 GB RAM and 3.3 GHz Xeon w-2155 CPU.

#### 5.5 Prediction Results for Different Urban Districts

We visualize the prediction errors and compare the predicted cases with the actual cases for each urban district in Figures 5, 6. As shown

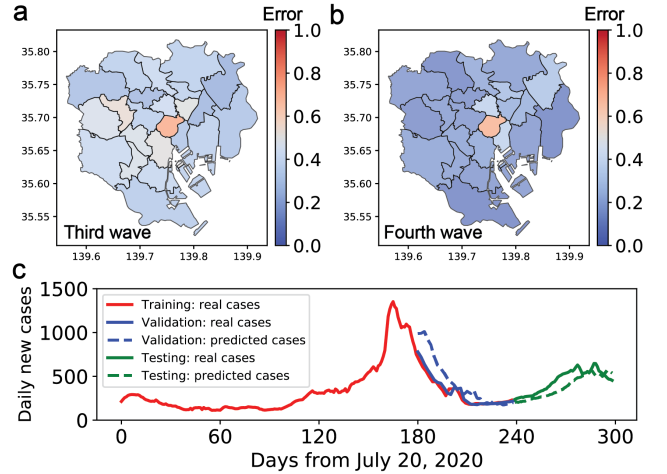


**Figure 5: Prediction performance of the SAB-GNN. (a,b) The relative prediction error (i.e.,  $|I_{real} - I_{predict}|/|I_{real}|$ ) during the third wave (a) and the fourth wave (b). (c) Predicted cases and real cases for the fourth wave when  $(D_1, D_2) = (21, 7)$ .**

in Figures 5ab, the relative prediction errors for most districts are homogeneously lower than 0.50 except for the central district (i.e., Chiyoda). This reveals that SAB-GNN mines the relationships between features and future infection cases in a global manner thanks to the message passing mechanism among neighborhood nodes.

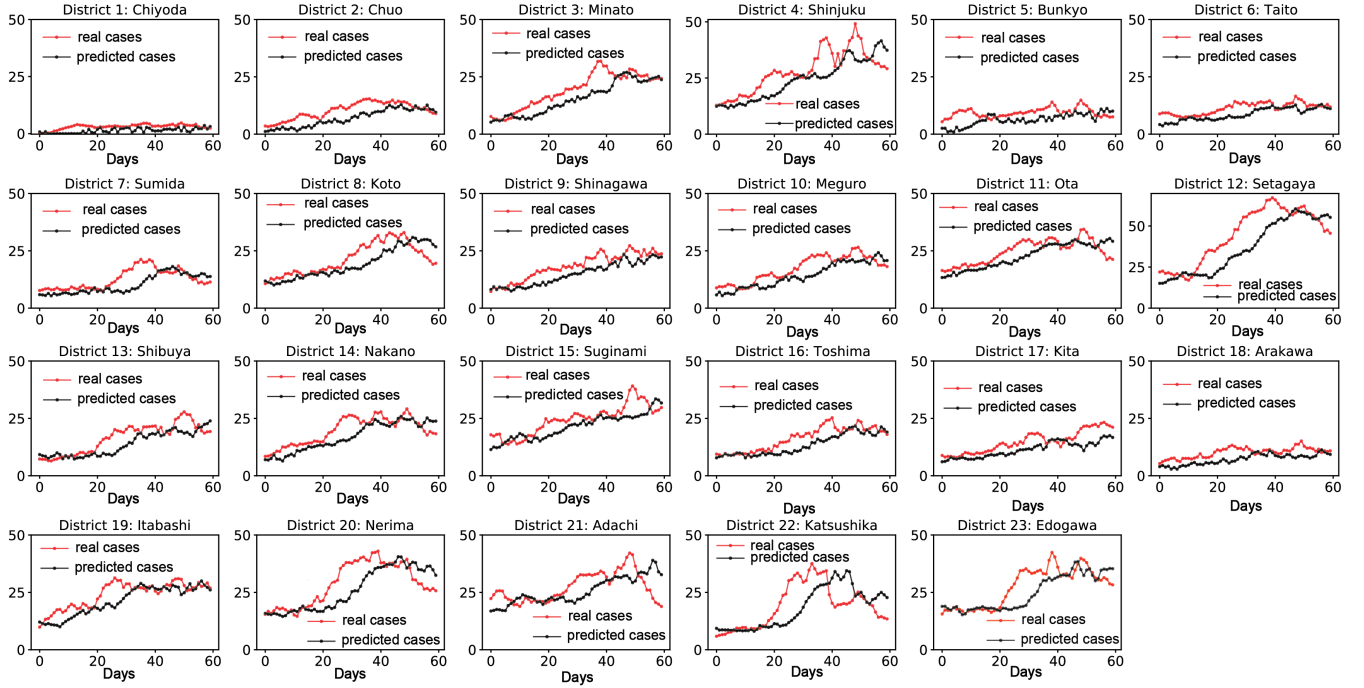


**Figure 6: Predicted and real cases on different urban districts of SAB-GNN for the fourth wave when  $(D_1, D_2) = (21, 7)$ .**

The reason for the relatively large prediction error in Chiyoda (i.e., District 1) is because Chiyoda is where Imperial Palace locates and has quite a few real infection cases (Figure 6). Figure 5c displays that the predicted daily case curve is able to capture the increasing tendency of actual cases from day 240 to day 280 and also maintains a small prediction error, which further demonstrates the power of our proposed SAB-GNN.

Figure 6 exhibits that for most urban districts, the model is able to anticipate the general increasing tendency of infection cases during the fourth wave. This information is especially valuable for local public agencies to make timely preparations at the beginning of a wave. Note that the prediction of District 4 (i.e., Shinjuku) is not as accurate as other districts. One potential interpolation is that Shinjuku is a commercial area with many entertainment industries and thus does not have similar infection patterns as other districts.

## 5.6 Parameter Sensitivity

The influences of model parameters in the SAB-GNN on the prediction performance are shown in Figure 7. Figure 7a displays the changes of RMSE for the fourth peak prediction with respect to varying numbers of symptom-related web search features used in the model. Note that there is a huge frequency discrepancy between different symptoms and we only feed the most frequent  $k$  symptoms into our model. The result suggests that  $k = 8$  provides the best prediction performance. The potential interpretation is that: when  $k$  is small, more symptoms contribute stronger connections with future infection cases; when  $k$  is large, many weakly-related symptoms bring noises to the training and thus harm the prediction performance.

Next, we tune the numbers of layers  $L_1, L_2$  in the GNN and LSTM modules (Figures 7bc) and conclude that  $(L_1, L_2) = (1, 2)$  yields the best prediction. It is reasonable that the simple model with a small number of parameters is preferred in this infection case prediction task whose training data is quite limited [36]. Finally, we test the model in Figure 7d by varying  $D_1$  and  $D_2$  and observe the overall tendency that using more days' (i.e.,  $D_1$  is large) information to predict later fewer days' (i.e.,  $D_2$  is small) results in higher accuracy, which is consistent with the finding from the existing study [32].

## 5.7 Ablation Study

To confirm the effect of each module in the SAB-GNN on prediction results, we perform the ablation experiments for both the third wave and fourth wave (Figure 8). We remove one of the three modules in the SAB-GNN, and perform the prediction for the same time horizons as the full SAB-GNN model. We show quantitatively that the SAB-GNN model obtains lower prediction RMSE than other incomplete models, especially for the third wave, which reveals that both the spatial module, temporal module, and social awareness module contribute to the final prediction results in a positive manner. While existing studies have paid much attention to the spatial and temporal relationships between features and infection cases, we recommend introducing suitable social knowledge into the prediction, given the positive effect of the social awareness recovery mechanism.

## 6 CONCLUSIONS

Motivated by the multiwave outbreak of COVID-19 across the globe, we establish the SAB-GNN to predict future infection cases. Besides



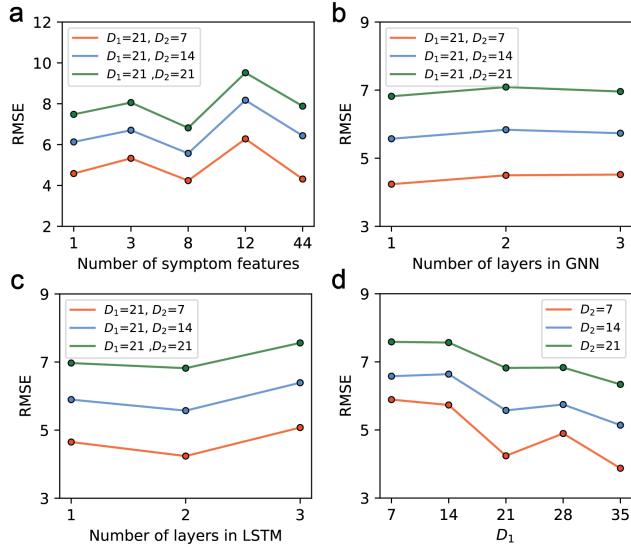


Figure 7: Parameter sensitivity study.

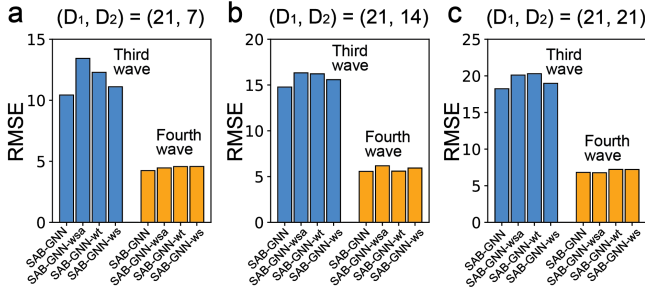


Figure 8: Ablation experiments. We implement the algorithms of SAB-GCN, SAB-GCN-wsa (without social awareness), SAB-GCN-wt (without temporal module), SAB-GCN-wws (without spatial module) for the third wave (the blue bar) and the fourth wave (the orange bar).

the historical infection and mobility data used in existing studies, our approach utilizes the novel symptom-related web search data which provides alternative evidence of future waves. More importantly, we consider the social awareness decay effect and propose the social awareness recovery module to estimate the actual infection risks. Experiments on the third and fourth peaks of Tokyo affirm that the SAB-GNN outperforms other baseline models and captures the increasing trend of pandemic waves. Our method is applicable to many countries given the wide coverage of web search data.

## REFERENCES

[1] Joost Bastings, Ivan Titov, Wilker Aziz, Diego Marcheggiani, and Khalil Sima'an. 2017. Graph Convolutional Encoders for Syntax-aware Neural Machine Translation. In *EMNLP*.

[2] Ana I Bento, Thuy Nguyen, Coady Wing, Felipe Lozano-Rojas, Yong-Yeol Ahn, and Kosali Simon. 2020. Evidence from internet search data shows information-seeking responses to news of local COVID-19 cases. *Proceedings of the National Academy of Sciences* 117, 21 (2020), 11220–11222.

[3] Giacomo Cacciapaglia, Corentin Cot, and Francesco Sannino. 2020. Second wave COVID-19 pandemics in Europe: a temporal playbook. *Scientific reports* 10, 1 (2020), 1–8.

[4] Centers for Disease Control and Prevention. 2021. Symptoms of COVID-19. <https://www.cdc.gov/coronavirus/2019-ncov/symptoms-testing/symptoms.html>.

[5] Serina Chang, Emma Pierson, Pang Wei Koh, Jaline Gerardin, Beth Redbird, David Grusky, and Jure Leskovec. 2020. Mobility network models of COVID-19 explain inequities and inform reopening. *Nature* (2020), 1–6.

[6] Serina Y Chang, Mandy L Wilson, Bryan Lewis, Zakaria Mehrab, Komal K Dudakiya, Emma Pierson, Pang Wei Koh, Jaline Gerardin, Beth Redbird, David Grusky, et al. 2021. Supporting COVID-19 policy response with large-scale mobility-based modeling. *medRxiv* (2021).

[7] Cen Chen, Kenli Li, Sin G Teo, Xiaofeng Zou, Kang Wang, Jie Wang, and Zeng Zeng. 2019. Gated residual recurrent graph neural networks for traffic prediction. In *Proceedings of the AAAI conference on artificial intelligence*, Vol. 33, 485–492.

[8] Yizong Cheng. 1995. Mean shift, mode seeking, and clustering. *IEEE transactions on pattern analysis and machine intelligence* 17, 8 (1995), 790–799.

[9] Vinay Kumar Reddy Chimmula and Lei Zhang. 2020. Time series forecasting of COVID-19 transmission in Canada using LSTM networks. *Chaos, Solitons & Fractals* (2020), 109864.

[10] Matteo Chinazzi. accessed August 2021. Mobility, commuting, and contact patterns across the United States during the COVID-19 outbreak. Available online at <https://covid19.gleamproject.org/mobility>.

[11] Kyunghyun Cho, Bart Van Merriënboer, Caglar Gulcehre, Dzmitry Bahdanau, Fethi Bougares, Holger Schwenk, and Yoshua Bengio. 2014. Learning phrase representations using RNN encoder-decoder for statistical machine translation. *arXiv preprint arXiv:1406.1078* (2014).

[12] Amelie Desvars-Larrive, Elma Dervic, Nils Haug, Thomas Niederkrotenthaler, Jiaying Chen, Anna Di Natale, Jana Lasser, Diana S Gliga, Alexandra Roux, Johannes Sorger, et al. 2020. A structured open dataset of government interventions in response to COVID-19. *Scientific data* 7, 1 (2020), 1–9.

[13] Junyi Gao, Rakshith Sharma, Cheng Qian, Lucas M Glass, Jeffrey Spaeder, Justin Romberg, Jimeng Sun, and Cao Xiao. 2021. STAN: spatio-temporal attention network for pandemic prediction using real-world evidence. *Journal of the American Medical Informatics Association* 28, 4 (2021), 733–743.

[14] Sharad Goel, Jake M Hofman, Sébastien Lahaie, David M Pennock, and Duncan J Watts. 2010. Predicting consumer behavior with Web search. *Proceedings of the National academy of sciences* 107, 41 (2010), 17486–17490.

[15] Google Inc. 2021. Covid-19 infection cases. <https://news.google.com/covid19/map?hl=en-US&gl=US&ceid=US%3Aen>.

[16] Will Hamilton, Zhitao Ying, and Jure Leskovec. 2017. Inductive representation learning on large graphs. In *Advances in neural information processing systems*, 1024–1034.

[17] Shohei Hisada, Taichi Murayama, Kota Tsubouchi, Sumio Fujita, Shuntaro Yada, Shoko Wakamiya, and Eiji Aramaki. 2020. Surveillance of early stage COVID-19 clusters using search query logs and mobile device-based location information. *Scientific Reports* 10, 1 (2020), 1–8.

[18] Sepp Hochreiter and Jürgen Schmidhuber. 1997. Long short-term memory. *Neural computation* 9, 8 (1997), 1735–1780.

[19] Xiao Huang, Zhenlong Li, Yuqin Jiang, Xiaoming Li, and Dwayne Porter. 2020. Twitter reveals human mobility dynamics during the COVID-19 pandemic. *PLoS one* 15, 11 (2020), e0241957.

[20] HyeonChan Jo, Juhyun Kim, Tzu-Chen Huang, and Yu-Li Ni. 2020. condLSTM-Q: A novel deep learning model for predicting Covid-19 mortality in fine geographical Scale. *arXiv preprint arXiv:2011.11507* (2020).

[21] Mingxuan Ju, Wei Song, Shiyu Sun, Yanfang Ye, Yujie Fan, Shifu Hou, Kenneth Loparo, and Liang Zhao. 2021. Dr. Emotion: Disentangled Representation Learning for Emotion Analysis on Social Media to Improve Community Resilience in the COVID-19 Era and Beyond. In *Proceedings of the Web Conference 2021*, 518–528.

[22] Yuhao Kang, Song Gao, Yunlei Liang, Mingxiao Li, Jinneng Rao, and Jake Kruse. 2020. Multiscale dynamic human mobility flow dataset in the US during the COVID-19 epidemic. *Scientific data* 7, 1 (2020), 1–13.

[23] Amol Kapoor, Xue Ben, Luyang Liu, Bryan Perozzi, Matt Barnes, Martin Blais, and Shawn O'Banion. 2020. Examining covid-19 forecasting using spatio-temporal graph neural networks. *arXiv preprint arXiv:2007.03113* (2020).

[24] Efthimios Kaxiras and Georgios Neofotistos. 2020. Multiple epidemic wave model of the covid-19 pandemic: Modeling study. *Journal of Medical Internet Research* 22, 7 (2020), e20912.

[25] Diederik P Kingma and Jimmy Ba. 2014. Adam: A method for stochastic optimization. *arXiv preprint arXiv:1412.6980* (2014).

[26] Thomas N Kipf and Max Welling. 2016. Semi-supervised classification with graph convolutional networks. *arXiv preprint arXiv:1609.02907* (2016).

[27] Stephen M Kissler, Christine Tedijanto, Edward Goldstein, Yonatan H Grad, and Marc Lipsitch. 2020. Projecting the transmission dynamics of SARS-CoV-2 through the postpandemic period. *Science* 368, 6493 (2020), 860–868.

[28] Tadeusz Kufel et al. 2020. ARIMA-based forecasting of the dynamics of confirmed Covid-19 cases for selected European countries. *Equilibrium. Quarterly Journal*

- of *Economics and Economic Policy* 15, 2 (2020), 181–204.
- [29] Kathy Leung, Joseph T Wu, Di Liu, and Gabriel M Leung. 2020. First-wave COVID-19 transmissibility and severity in China outside Hubei after control measures, and second-wave scenario planning: a modelling impact assessment. *The Lancet* 395, 10233 (2020), 1382–1393.
  - [30] Seyed M Moghadas, Affan Shoukat, Meagan C Fitzpatrick, Chad R Wells, Pratha Sah, Abhishek Pandey, Jeffrey D Sachs, Zheng Wang, Lauren A Meyers, Burton H Singer, et al. 2020. Projecting hospital utilization during the COVID-19 outbreaks in the United States. *Proceedings of the National Academy of Sciences* 117, 16 (2020), 9122–9126.
  - [31] Medhini Narasimhan, Svetlana Lazebnik, and Alexander G Schwing. 2018. Out of the box: Reasoning with graph convolution nets for factual visual question answering. *Advances in Neural Information Processing Systems* 2018 (2018), 2654–2665.
  - [32] George Panagopoulos, Giannis Nikolentzos, and Michalis Vazirgiannis. 2021. Transfer Graph Neural Networks for Pandemic Forecasting. In *Proceedings of the AAAI Conference on Artificial Intelligence*, Vol. 35. 4838–4845.
  - [33] Hao Peng, Hongfei Wang, Bowen Du, Md Zakirul Alam Bhuiyan, Hongyuan Ma, Jianwei Liu, Lihong Wang, Zeyu Yang, Linfeng Du, Senzhang Wang, et al. 2020. Spatial temporal incidence dynamic graph neural networks for traffic flow forecasting. *Information Sciences* 521 (2020), 277–290.
  - [34] Xinwu Qian, Lijun Sun, and Satish V Ukkusuri. 2021. Scaling of contact networks for epidemic spreading in urban transit systems. *Scientific reports* 11, 1 (2021), 1–12.
  - [35] Xinwu Qian, Jiawei Xue, and Satish V Ukkusuri. 2020. Modeling disease spreading with adaptive behavior considering local and global information dissemination. *arXiv preprint arXiv:2008.10853* (2020).
  - [36] Yu Qiu, Yun Liu, Shijie Li, and Jing Xu. 2021. MiniSeg: An Extremely Minimum Network for Efficient COVID-19 Segmentation. In *Proceedings of the AAAI Conference on Artificial Intelligence*, Vol. 35. 4846–4854.
  - [37] Alexander Rodriguez, Nikhil Muralidhar, Bijaya Adhikari, Anika Tabassum, Naren Ramakrishnan, and B Aditya Prakash. 2021. Steering a Historical Disease Forecasting Model Under a Pandemic: Case of Flu and COVID-19. In *Proceedings of AAAI*.
  - [38] Abeer Sarker, Sahithi Lakamana, Whitney Hogg-Bremer, Angel Xie, Mohammed Ali Al-Garadi, and Yuan-Chi Yang. 2020. Self-reported COVID-19 symptoms on Twitter: an analysis and a research resource. *Journal of the American Medical Informatics Association* 27, 8 (2020), 1310–1315.
  - [39] Michael Schlichtkrull, Thomas N Kipf, Peter Bloem, Rianne Van Den Berg, Ivan Titov, and Max Welling. 2018. Modeling relational data with graph convolutional networks. In *European Semantic Web Conference*. Springer, 593–607.
  - [40] Amray Schwabe, Joel Persson, and Stefan Feuerriegel. 2021. Predicting COVID-19 Spread from Large-Scale Mobility Data. In *KDD 2021*.
  - [41] Farah Shahid, Aneela Zameer, and Muhammad Muneeb. 2020. Predictions for COVID-19 with deep learning models of LSTM, GRU and Bi-LSTM. *Chaos, Solitons & Fractals* 140 (2020), 110212.
  - [42] Tokyo COVID-19 Task Force Website. 2021. Covid-19 infection cases. <https://github.com/codeforshinjuku/covid19/blob/master/dist/patient.json>.
  - [43] Petar Veličković, Guillem Cucurull, Arantxa Casanova, Adriana Romero, Pietro Lio, and Yoshua Bengio. 2017. Graph attention networks. *arXiv preprint arXiv:1710.10903* (2017).
  - [44] Jingqi Wang, Noor Abu-el Rub, Josh Gray, Huy Anh Pham, Yujia Zhou, Frank J Manion, Mei Liu, Xing Song, Hua Xu, Masoud Rouhizadeh, et al. 2021. COVID-19 SignSym: a fast adaptation of a general clinical NLP tool to identify and normalize COVID-19 signs and symptoms to OMOP common data model. *Journal of the American Medical Informatics Association* 28, 6 (2021), 1275–1283.
  - [45] Lijing Wang, Aniruddha Adiga, Srinivasan Venkatramanan, Jiangzhuo Chen, Bryan Lewis, and Madhav Marathe. 2020. Examining Deep Learning Models with Multiple Data Sources for COVID-19 Forecasting. In *2020 IEEE International Conference on Big Data (Big Data)*. IEEE, 3846–3855.
  - [46] Xiaoyang Wang, Yao Ma, Yiqi Wang, Wei Jin, Xin Wang, Jiliang Tang, Caiyan Jia, and Jian Yu. 2020. Traffic flow prediction via spatial temporal graph neural network. In *Proceedings of The Web Conference 2020*. 1082–1092.
  - [47] Zifeng Wang, Rui Wen, Xi Chen, Shilei Cao, Shao-Lun Huang, Buyue Qian, and Yefeng Zheng. 2021. Online Disease Diagnosis with Inductive Heterogeneous Graph Convolutional Networks. In *Proceedings of the Web Conference 2021*. 3349–3358.
  - [48] Congxi Xiao, Jingbo Zhou, Jizhou Huang, An Zhuo, Ji Liu, Haoyi Xiong, and Dejing Dou. 2021. C-Watcher: A Framework for Early Detection of High-Risk Neighborhoods Ahead of COVID-19 Outbreak. In *Proceedings of the AAAI Conference on Artificial Intelligence*, Vol. 35. 4892–4900.
  - [49] Chenfeng Xiong, Songhua Hu, Mofeng Yang, Weiyu Luo, and Lei Zhang. 2020. Mobile device data reveal the dynamics in a positive relationship between human mobility and COVID-19 infections. *Proceedings of the National Academy of Sciences* 117, 44 (2020), 27087–27089.
  - [50] Jiawei Xue, Nan Jiang, Senwei Liang, Qiyuan Pang, Satish V Ukkusuri, and Jianzhu Ma. 2021. Quantifying spatial homogeneity of urban road networks via graph neural networks. *arXiv preprint arXiv:2101.00307* (2021).
  - [51] Takahiro Yabe, Kota Tsubouchi, Naoya Fujiwara, Takayuki Wada, Yoshihide Sekimoto, and Satish V Ukkusuri. 2020. Non-compulsory measures sufficiently reduced human mobility in Tokyo during the COVID-19 epidemic. *Scientific reports* 10, 1 (2020), 1–9.
  - [52] Takahiro Yabe, Kota Tsubouchi, and Satish V Ukkusuri. 2020. Early Warning of COVID-19 Hotspots using Mobility of High Risk Users from Web Search Queries. *arXiv preprint arXiv:2010.13254* (2020).
  - [53] Rui Yan, Weiheng Liao, Jianwei Cui, Hailei Zhang, Yichuan Hu, and Dongyan Zhao. 2021. Multilingual COVID-QA: Learning towards Global Information Sharing via Web Question Answering in Multiple Languages. In *Proceedings of the Web Conference 2021*. 2590–2600.
  - [54] Huaxiu Yao, Xianfeng Tang, Hua Wei, Guanjie Zheng, and Zhenhui Li. 2019. Revisiting spatial-temporal similarity: A deep learning framework for traffic prediction. In *Proceedings of the AAAI conference on artificial intelligence*, Vol. 33. 5668–5675.
  - [55] Huaxiu Yao, Fei Wu, Jintao Ke, Xianfeng Tang, Yitian Jia, Siyu Lu, Pinghua Gong, Jieping Ye, and Zhenhui Li. 2018. Deep multi-view spatial-temporal network for taxi demand prediction. In *Proceedings of the AAAI Conference on Artificial Intelligence*, Vol. 32.
  - [56] Yanfang Ye, Shifu Hou, Yujie Fan, Yiming Zhang, Yiyue Qian, Shiyu Sun, Qian Peng, Mingxuan Ju, Wei Song, and Kenneth Loparo. 2020. *alpha*-Satellite: An AI-Driven System and Benchmark Datasets for Dynamic COVID-19 Risk Assessment in the United States. *IEEE Journal of Biomedical and Health Informatics* 24, 10 (2020), 2755–2764.
  - [57] Xiyue Zhang, Chao Huang, Yong Xu, Lianghao Xia, Peng Dai, Liefeng Bo, Junbo Zhang, and Yu Zheng. 2021. Traffic Flow Forecasting with Spatial-Temporal Graph Diffusion Network. In *Proceedings of the AAAI Conference on Artificial Intelligence*, Vol. 35. 15008–15015.
  - [58] Xu Zhong and Michael Raghieb. 2019. Revisiting the use of web search data for stock market movements. *Scientific reports* 9, 1 (2019), 1–8.
  - [59] Feng Zhou, Tao Chen, and Baiying Lei. 2020. Do not forget interaction: Predicting fatality of COVID-19 patients using logistic regression. *arXiv preprint arXiv:2006.16942* (2020).
  - [60] Jie Zhou, Ganqu Cui, Shengding Hu, Zhengyan Zhang, Cheng Yang, Zhiyuan Liu, Lifeng Wang, Changcheng Li, and Maosong Sun. 2020. Graph neural networks: A review of methods and applications. *AI Open* 1 (2020), 57–81.